



## City Research Online

### City, University of London Institutional Repository

---

**Citation:** Javdani, S., Fabian, M., Carlton, J., Sun, T. & Grattan, K. T. V. (2016). Underwater free-vibration analysis of full-scale marine propeller using a Fibre Bragg Grating-based sensor system. *IEEE Sensors Journal*, 16(4), pp. 946-953. doi: 10.1109/jsen.2015.2490478

This is the accepted version of the paper.

This version of the publication may differ from the final published version.

---

**Permanent repository link:** <https://openaccess.city.ac.uk/id/eprint/12797/>

**Link to published version:** <https://doi.org/10.1109/jsen.2015.2490478>

**Copyright:** City Research Online aims to make research outputs of City, University of London available to a wider audience. Copyright and Moral Rights remain with the author(s) and/or copyright holders. URLs from City Research Online may be freely distributed and linked to.

**Reuse:** Copies of full items can be used for personal research or study, educational, or not-for-profit purposes without prior permission or charge. Provided that the authors, title and full bibliographic details are credited, a hyperlink and/or URL is given for the original metadata page and the content is not changed in any way.

---

City Research Online:

<http://openaccess.city.ac.uk/>

[publications@city.ac.uk](mailto:publications@city.ac.uk)

---

# Underwater free-vibration analysis of full-scale marine propeller using a Fibre Bragg Grating-based sensor system

Saeed Javdani, Matthias Fabian, John S. Carlton, Tong Sun, and Kenneth T. V. Grattan

**Abstract**—A detailed study has been carried out on instrumented, full-scale marine propeller blades in order to investigate their vibration behaviour, both in air and underwater. In order to do so and to obtain data with minimum perturbation to the characteristics of the blades, a Fibre Bragg Grating-based sensor network system was designed and implemented, for the first time. The individual vibration frequencies at each measurement point and thus the broader vibration patterns seen for each of the blades were obtained, with excitation both in air and in water and the results are compared to those obtained from Finite Element (FE) analysis. The vibration patterns obtained show that the same modes of vibration occur in air and in water, although in some natural frequencies the mode order is seen to change from one blade to another on the same propeller.

The extensive performance survey carried out has also shown that while the effect of the added mass of water on the natural frequencies of the blades in the fundamental modes is considerable, this effect diminishes as the natural frequencies of the blades increase. The results obtained from the optical fibre sensor network were compared to those from previous work in this area using different and less satisfactory techniques and it was confirmed that the ratio of the natural frequencies in water to those in air increases in a linear manner as the frequencies were increasing. Additionally, the natural frequencies of a blade were measured under different depths of propeller immersion.

**Index Terms**—Fibre Bragg Grating (FBG)-based sensor network, full-scale propeller, vibration sensor, mode shape, natural frequency

## I. INTRODUCTION

The research described in this paper forms part of an ongoing investigation into achieving better means of measurement of the vibrational characteristics of full-scale marine propellers, both in air and under water, and thus to achieve a better understanding of their performance by comparing the results obtained from experimental measurements with the outputs of advanced numerical analysis. To do so, the effectiveness and accuracy of a FBG-based multi-sensor system which had been designed specifically for the purpose and implemented was investigated and examined. The aim has been to achieve a more accurate measurement of the frequencies and modes of vibration of the complex geometries that particularly characterize large marine propeller blades. The key purpose underpinning the tests carried out was to provide better answers to the key questions posed by the marine industry in the characterization of such propeller blades – to understand, for example, the effect of added mass of water on the frequencies and modes of vibration of these propeller blades, of modern design and manufacture and considerable unit cost.

In the case of marine propellers, blades rotate slowly compared for example to blades in fans, jets and in turbines and hence, the centrifugal forces on the blades and therefore the stiffness increase that would result can be ignored, as it is minimal. In a series of experiments and subsequent

calculations carried out by Conn [1], it was concluded that it is mainly the flexural frequencies that are affected by the centrifugal forces. The flexural frequencies of a rotating blade can be calculated from the following relationship:

$$f^2 = f_0^2 + k\Omega^2 \quad (1)$$

where  $f$  is natural frequency of the rotating blade (Hz),  $f_0$  is the natural frequency of a non-rotating blade,  $\Omega$  is the angular velocity (in revolutions per second (rps), this normally having a value of around 5 to 10 in the case of marine propellers) and  $k$  is a constant which has the values 0.35 and 1.35 for vibration parallel and perpendicular to the blade breadths. It can be seen from the relationship that the effect of rotation on the frequencies of the blades is negligible. This was confirmed in work carried out by Castellini and Santolini [2], where they measured the natural frequencies of a small-scale, *model* propeller underwater using a non-contact tracking laser vibrometer. They concluded that under rotating conditions, the bending modes were observed to be the most important vibration modes, since excitation due to hydrodynamic effects, gas bubbles or cavitation induces hardly any torsion effects on the blade structure.

The principal effect of immersing a propeller in water is to cause a reduction in the frequencies at the particular mode at which the vibration occurs. However, this reduction is not constant and appears to be greater for lower modes of vibration, when compared to higher modes. In order to investigate this effect, Carlton [3] has defined the frequency reduction ratio as

$$\Lambda = \frac{\text{frequency of mode in water}}{\text{frequency of mode in air}} \quad (2)$$

Considering a blade as a system with a single degree of freedom, the relationship between the motion of such a system under an undamped situation (while the stiffness remains unchanged) can be presented as a simple mass ratio equation, as shown in equation 3:

$$\Lambda = \left( \frac{M_b}{M_b + M_w} \right)^{\frac{1}{2}} \quad (3)$$

where  $M_b$  is the equivalent mass of the blade and  $M_w$  is the added mass of water.

A previous investigation by Burrill into this relationship on model and full scale propellers, references [4 and 5], showed that the value of  $\Lambda$  increases with the modal number, as illustrated in Table 1.

Looking at a propeller with a higher blade area ratio (BAR = 0.85), the work of Hughes [6] has confirmed the results obtained by Burrill which show an increase in the values of  $\Lambda$  with increasing the mode number. It has also been shown by Burrill and Hughes and others [7 and 8] that changes in mode

shapes of vibration due to immersion in water are generally small, although a shift in position of the modal lines on the blade can be seen in some modes, as illustrated in Figure 1.

**Table 1. The effect on modal frequency of immersion in water for a four-bladed propeller with a Blade Area Ratio (BAR) of 0.526 and Mean Pitch (P/D) of 0.65**

Flexural vibration modes	Frequency (Hz)		$\Delta$
	In air	In Water	
Fundamental	160	100	0.625
One-node mode	230	161	0.700
Two-node mode	460	375	0.815
Three-node mode	710	625	0.880
Four-node Mode	1020	1000	0.980
<i>Torsional vibration modes</i>			
One-node mode	400	265	0.662
Two-node mode	670	490	0.731
Three-node mode	840	-	-

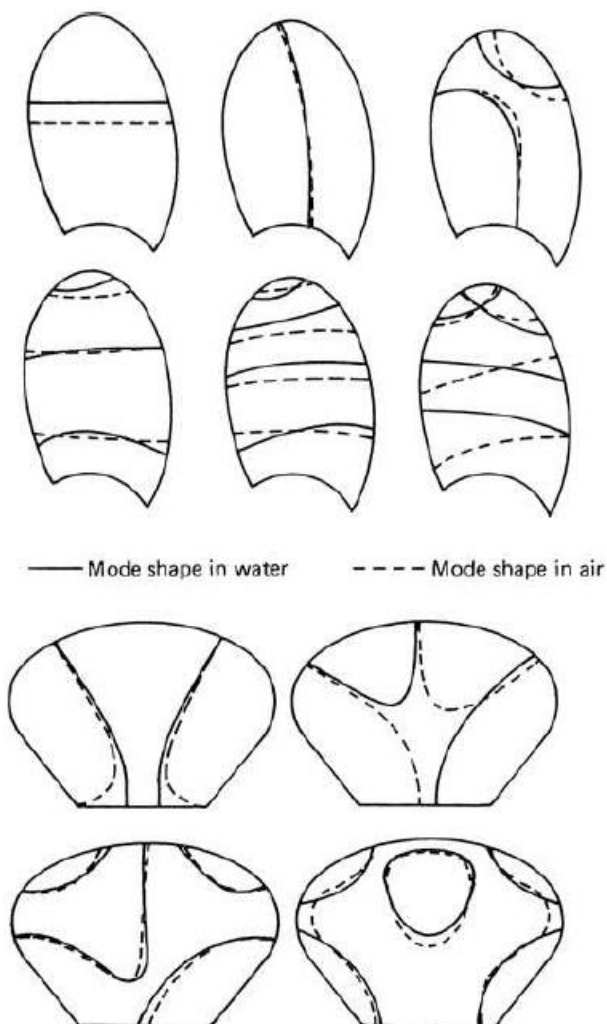


Fig. 1. Mode shapes in air and water for the two different propeller forms and Blade Area Ratio (BAR). Source: Carlton 2012 [3]

The present work seeks to make a significant advance on work previously reported and thus is a study of the application of a FBG-based sensor network system for the direct acquisition of natural frequencies and mode shapes of vibrations of a full-scale marine propeller of modern design in

water and in air. The FBG-based sensors show the major advantages of being minimally invasive on the blade itself and its performance, whilst allowing a very large number of sensing points to be investigated, unlike the use of for example electronic strain gauges. Further, these FBG-based sensors can be applied with a high degree of dimensional precision ( $\pm 1\text{mm}$ ) to those points on the blades where measurements are desired and measurements from all the sensing points could, in principle, be obtained simultaneously. There is no electrical hazard with the use of these sensors in air, or more particularly in highly conductive sea water, unlike the case with electronic strain gauges and when comparing to the use of non-contact laser-based methods to target specific points (usually one-by-one) in water, there is no need to consider refractive effects on the probe light when attempting to direct a laser beam with high precision to a specific part of the surface of blade – indeed there is no need for the blade to be visible to the operator.

## II. EXPERIMENTAL ASPECTS

The propeller selected for investigation in this experiment is a left-handed propeller designed for a twin-screw ship. The fixed pitch propeller blades had a diameter of 1900 mm with a variable pitch distribution of the blade. Table 2 presents the principal characteristics of propeller blade geometry and the material properties of the propeller. Figure 2 shows a photograph of the propeller immersed in a water tank of base size 4x4 meters (and wall height of 2 meters), as used in this experiment with the blades instrumented with the optical FBG-based sensor network designed for this work, showing the minimally-invasive nature of the >300 sensors attached to the propeller used for this test.

**Table 2. Characteristics of propeller in this experiment**

Diameter,	1900 mm
Mean Pitch	1631 mm
Expanded Area Ratio	0.765
Modulus of Elasticity, E	121 GPa
Poisson Ratio, $\nu$	0.33
Density, $\rho$	7650 kg.m <sup>3</sup>

The FBG-based sensors used as the basis of each sensor element were as follows. Each individual sensor was created using a Type I FBG (of 6 mm length), fabricated using the conventional zero-order nulled diffraction phase mask technique [9]. To do so, 248 nm laser pulses (12 mJ at 300 Hz) from an ATLEX-300-SI Excimer laser were focussed via a 20 mm focal length plano-cylindrical lens through a series of commercially available phase masks (Oe-land, QPS) into the core of a photosensitive fibre (Fibercore PS1250). The sensors were configured into a number of individual channels for convenience and to minimize the number of external optical fibre leads coming from the blade (as can be seen from Figure 2). Thus in each channel seven different FBG wavelengths, set to be between 1525 nm and 1565 nm were chosen, to ensure that there was no spectral overlap from one sensor to the next, even when each sensor responds over its maximum range of vibration-induced strain to avoid any ambiguity in the measurement. These FBG-based channels then formed the

network of sensors on each blade – a pattern that was repeated for each of the five blades of the propeller.

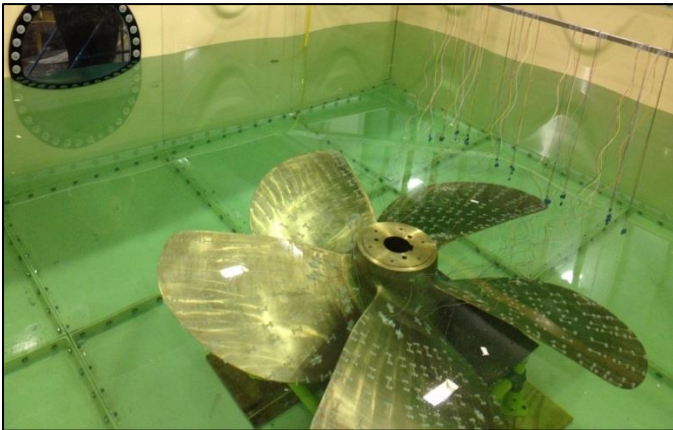


Fig. 2. Left-handed propeller in water tank; 5 blades instrumented with a network of 67 sensors attached onto each blade. The total number of FBG-based sensors used on the propeller was 335.

The dynamic Bragg wavelength shifts, monitored from each FBG from all the channels comprising the entire sensor network and caused by the vibrations detected when the propeller blades were excited were captured simultaneously using a Micron Optics SM130-700 sensing interrogator unit, operating at a sampling rate of 2000 Hz. In processing these signals, all the DC components were then removed from the transient signals before a Fast Fourier Transform (FFT) algorithm was applied to extract the frequency components from each of the sensor data sets, with the maximum detectable vibration frequency being 1000 Hz (half the sampling rate). In order to determine the most significant spectral features for all frequencies in the FFT spectra detected, the sampling interval was chosen to be 2 s. In tests carried out, longer sampling intervals were found not to be beneficial as they resulted in lower amplitudes for the higher frequencies detected, as they typically dampen faster than low frequency vibrations. **This sampling interval (2 seconds) resulted in maximum detectable vibration frequency being 900Hz.** The frequency resolution,  $\Delta f$ , of the FFT spectra depends on the sampling frequency,  $f_s$ , and the number of sample values,  $N$ , taken (where  $\Delta f = f_s/N$ ), where  $N$  is a product of the sampling frequency and the sampling interval  $t_s$ . Thus,  $\Delta f = 1/t_s = 0.5$  Hz for the chosen sampling interval of 2 s. A band-pass filtering approach was also applied to tenable the relative wavelength shifts measured at each point where a FBG-based sensor was mounted to be tracked, showing the natural frequencies of there and thus to obtain the strain mode profile of the blade at that specific frequency. For each of the detected frequency components, the amplitudes and relative wavelength shifts at the different sensor locations were then used to plot the deflection charts (the mode maps) for each blade.

To create a sufficient pattern of frequency information in the experiment carried out, each blade was instrumented with a 10 channel network of sensors on the fibre, with each containing between 5-7 FBG-based sensors (depending on the shape of the blade at that position), each using different wavelengths to allow individual sensor identification. The FBG spectral characteristics were each centred at a specific, known wavelength in the spectral region between 1525 nm and 1565 nm and they were written into optical fibres channels,

each of lengths between 450 mm to 900 mm to suit the position on which they were mounted on the blade, in the manner as was discussed earlier. The sensor locations on the expanded outline of the one of the blade surfaces is shown in Figure 3 – this pattern was repeated for all five blades as they were similar in shape and size.

Each of the sensors in the optical fiber channels used was attached to the blade surface, in a way designed to be as far as possible normal to the chordal lines, to enable the results obtained from any individual sensor to be as closely comparable to those obtained from the other sensors. The modes of vibration of the blades, in air, were excited by striking the blades at various known locations on the propeller with a hammer with a relatively hard rubber tip, in order to excite the vibration of the blade across the full vibrational frequency range. Since the sensing interrogator unit was able to read data from 4 fibres simultaneously, first the optical fibre array next to the trailing edge of the blades was used as a reference for normalizing the captured amplitudes of the strain data. Therefore, when capturing data in this way, a series of three tests was necessary to obtain all the data for all the sensing locations for the blade shown in Figure 3. This was not difficult to do quickly and reproducibly. Then the amplitudes determined from the data from each set of tests were normalized to those obtained from the 1<sup>st</sup> sensor of the first fibre array, to allow the amplitude then to be comparable.

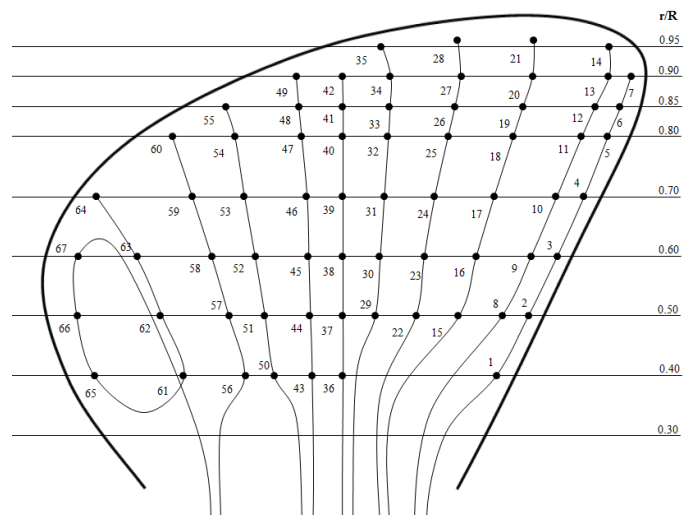


Fig. 3. Schematic of the instrumented propeller blade showing the sensor location points (numbered) as used for the optical sensor vibrational analysis, using the Fibre Bragg Grating-based sensor network. The sensor locations are shown in an expanded view of one of the blades.

Mode orders were tracked using a strain mode shape-based (SMSB) method. Hence the strain mode shapes were generated using the normalized data obtained from each sensor location and the results were mapped onto an expanded surface of the blade and cross-compared with data obtained from across the different blades. In order to compare the experimental results with those from a simulation carried out, these results were then compared to those obtained from an extensive Finite Element (FE) analysis, carried out using Abaqus software. This is discussed below.

### III. SIMULATION SETUP AND RESULTS

In the simulation carried out, in order to obtain the eigenfrequencies and the mode shapes in water, an Acoustic Fluid-Structure Coupling (AFSC) approach was used. Since the vibration amplitudes are small, a linear theory can be applied, and as the water is quiescent, the influence of fluid viscosity and the shear layers are negligible. Thus the Fluid-Structure Interaction (FSI) technique, using acoustic elements, can be applied efficiently to compute the natural frequencies of the blades. For a coupled fluid-structure interaction problem, the fluid pressure load acting at the interface can be added to the structure equation of motion as follows:

$$[M_e]\{\ddot{u}_e\} + [C_e]\{\dot{u}_e\} + [K_e]\{u_e\} = \{F_e\} + \{F_e^{pr}\} \quad (4)$$

where  $M_e$  is the structural mass matrix,  $C_e$  is the structural damping matrix,  $K_e$  is the structural stiffness matrix,  $u_e$  is the nodal displacement vector,  $F_e$  is the structural load vector and  $F_e^{pr}$  is the fluid pressure load vector at the interface. In the case of coupled modal analysis, the water pressure could be described by use of the Helmholtz acoustic wave equation:

$$\nabla^2 p = \frac{1}{c^2} \frac{\partial^2 p}{\partial t^2} \quad (5)$$

where  $c$  is the acoustic wave speed ( $c^2 = k/\rho$ , in which  $k$  is the fluid bulk modulus and  $\rho$  is the fluid density);  $p$  is acoustic pressure,  $t$  is time and  $\nabla^2$  the Laplace operator. At the interface between the blade surface and the water, the relationship between the normal pressure gradient of the fluid and the normal acceleration of the structure is governed by the following equation [10]:

$$\{n\} \cdot \{\nabla p\} = -\rho_0 \{n\} \cdot \frac{\partial^2 U}{\partial t^2} \quad (6)$$

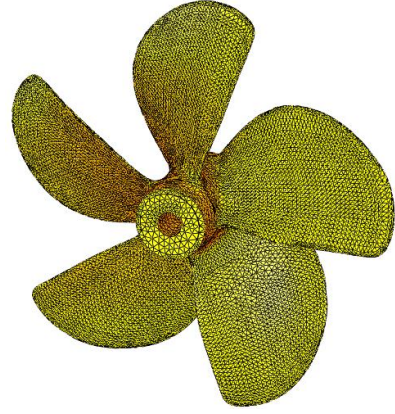
where  $U$  is the displacement vector of the interface of the structure and  $\rho_0$  is the density of the fluid. From the above equations, a complete set of finite element discretized equations for the fluid-structure interaction problem can be derived; it is, however, not the purpose of this paper to discuss the details of the finite element formulation of FSI modeling (further information can be found in theory manual of Abaqus package).

In order to ensure accuracy of the profile of each blade used in the simulation, for the FE modelling purposes for the full-scale propeller in the simulation package, the actual propeller was scanned using an industrial 3D scanning device and the point cloud data generated were transformed into surface bodies to provide the CAD model which could then be imported in Abaqus software for modal analysis. It was not possible to take advantage of the cyclic symmetry condition in this simulation since the manufactured blades have small discrepancies in their geometry which must be reflected in the model as they affect their natural frequencies in an important way- measuring these differences is an important feature of the approach taken in this work. Therefore, the full propeller had to be simulated to provide the data needed on its properties. For the modal analysis in air, the structure of the propeller was

'meshed' (that is a mesh grid was established covering the structure) with 3D tetrahedral elements of type C3D10. The full discretized model contained 90154 nodes and 51739 elements and the modal characteristics of the blades were obtained using the Block-Lanczos method in Abaqus. Figure 4a shows a schematic of the grids used for the analysis of the full propeller.

A major advantage of the use of the FBG-based sensors is the ability to monitor the performance in water, as well as air and thus to conduct a full simulation of the propeller in water, the same FE model of the full propeller was modified, this time adding the effect of the surrounding fluid domain to the model. The propeller was simulated in a water cylinder of diameter equal to  $1.25 \times$  the propeller diameter and height of 1000 mm. These dimensions were derived from preliminary measurements made in water and a number of simulations carried out and they were found to be sufficient to represent the surrounding water in the experimental setup. Figure 4b shows the propeller CAD model and water domain used in this simulation.

a)



b)

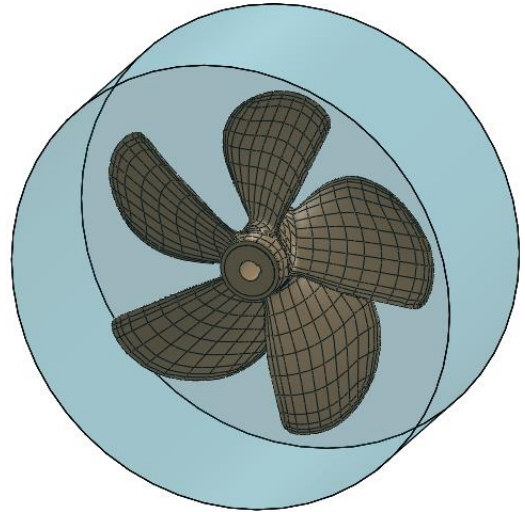


Fig. 4. a) FE model of the full propeller CAD model; b) propeller simulated in a cylindrical water domain.

Three-dimensional acoustic elements of type AC3D10 were used to mesh the fluid domain. The number of nodes and elements generated in the fluid domain were 291954 and 192552 respectively. The water properties necessary for this simulation were as follows: density  $\rho = 1000 \text{ kg/m}^3$  and bulk modulus = 2.15 GPa. The natural frequency and mode shapes obtained for the first 5 modes in air and in water were compared in Table 3 and Figure 5 respectively. Simulation

could be repeated for sea water, having a slightly different fluid density and bulk modulus. However, the results will not change notably.

As shown in Table 3a, although the natural frequencies of the blades are similar in terms of their fundamental modes, due to small geometrical discrepancies in each of the blades, the frequency difference that result from a similar excitation of each of the five blades studied are greater (with a difference of <15 Hz seen ) for some of the higher modes in air. However, it is interesting to note that this deviation is somewhat less pronounced for those modes in water. As would be expected, the frequency of a mode is seen to decrease in water.

**Table 3. Natural frequencies of 5 blades in air and water**

a) Left-handed Propeller Frequency Range (Hz); in air					
Mode No.	1	2	3	4	5
Blade 1	91.3	206.5	222.7	356.6	395.3
Blade 2	90.7	208.4	220.7	370.1	390.1
Blade 3	90.3	207.2	224.4	366.2	396.3
Blade 4	88.5	209.3	225.7	367.8	402.8
Blade 5	90.1	210.1	225.3	368.7	398.1

b) Left-handed Propeller Frequency Range (Hz); in water					
Mode No.	1	2	3	4	5
Blade 1	51.5	131.1	148.0	240.6	283.7
Blade 2	51.3	134.5	148.7	251.5	284.9
Blade 3	50.8	133.7	149.5	246.6	282.7
Blade 4	50.6	135.3	151.8	251.0	288.8
Blade 5	50.7	134.2	149.8	248.4	281.4

The mode shapes of the vibration simulated in water were seen to be similar for the first 5 modes simulated in air, as presented diagrammatically in Figure 5 for all the blades studied. However, the mode orders of the blades with closely-matched natural frequencies have been observed to be different in air and in water. For example, blade 5 has a higher natural frequency in air when compared to blade 4, in terms of the fourth mode order (Mode No. 4), while having a lower natural frequency in water.

A comparison is made with results reported in the literature. The results of this simulation (for frequencies up to the 12<sup>th</sup> mode order) and those reported by Hughes [6] show the linearity of the frequency reduction ratio ( $\Lambda$ ) of the natural frequency in water, compared to what is seen in air. An interesting observation from the simulation was that the frequency ratio increases up to mode 6 for all the blades and then drops at mode 7 perhaps due to a more complex mode of vibration at this mode. Complexity of vibrational modes increases the effect of added mass of water resulting in a lower frequency reduction ratio, and this increasing trend seems likely to continue beyond mode 7. This trend is also similar to what is seen in the results reported by Hughes, where there the peak in the frequency ratio is compared for mode 6, with the result shown in Figure 6. This peak appears at mode 4 in the results reported by Burrill [4 and 5] and reproduced in Table 1.

These agreements give confidence in the simulation carried out in this work.

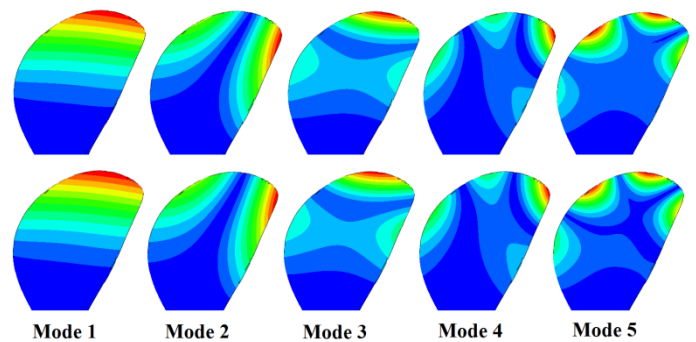


Fig. 5. Illustration of the mode shapes of the first 5 natural frequencies for blade 5 of the propeller studied in this simulation. Top row shows the mode patterns obtained in air and the bottom row are those captured in water.

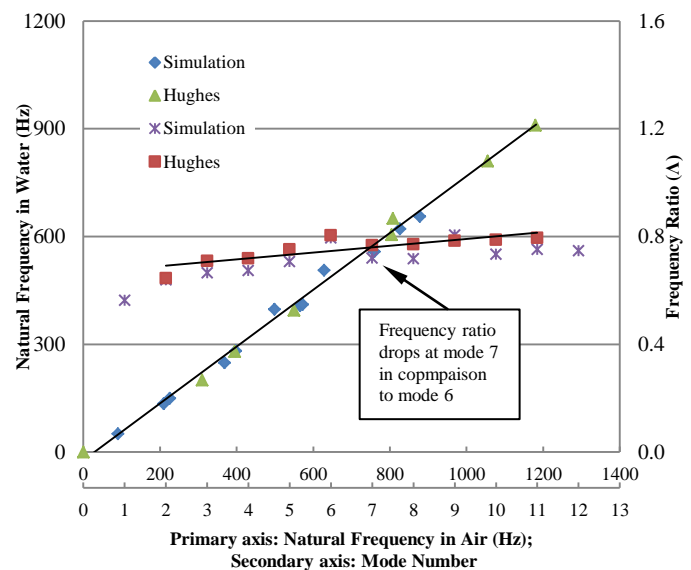


Fig. 6. Simulation of the effect of immersion on the natural frequencies. The line with lower slope shows the frequency ratio ( $\Lambda$ ) for different mode numbers. The second line shows the linear effect of immersion on natural frequencies. Mode 6 has a peak frequency ratio in neighbouring mode numbers.

#### IV. EXPERIMENTAL RESULTS AND DISCUSSION

Building on the above confidence in the simulation carried out and before undertaking the experimental vibration tests in water, it was necessary to determine the required water level to be used above the propeller blade, so that the natural frequencies are not affected by the depth of immersion. A deep tank was available in which to undertake these measurements and hence a series of preliminary tests was carried out using different water levels, namely 1350mm, 1450 mm and 1550mm, measured for convenience from the bottom of the water tank. The propeller in these tests was placed on a solid base of height 500 mm from the bottom of the tank, leaving the propeller blades to be immersed in 425mm, 475mm and 525 mm of water respectively from the free water surface. Further, tests were performed on the steady blades excited via impact hammer. The results of these preliminary tests for a representative blade, Blade 3, are shown in Figure 7. It can be seen from the results in this figure that increasing the water

level from 1350 mm to 1550 mm does not affect the natural frequencies measured. Therefore it was considered unnecessary to increase the water level further and it was thus decided to conduct further tests in the tank using a 1350 mm water level.

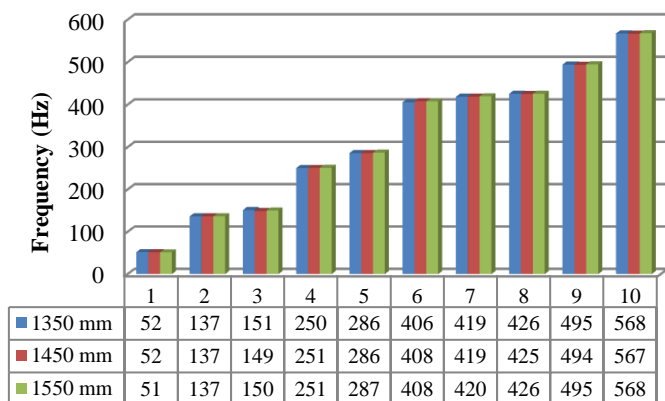


Fig. 7. Natural frequencies measured at different water levels (shown below the x-axis). Natural frequencies (Hz) up to the 10<sup>th</sup> mode (the top numbers on the x-axis) are presented in the table, for three different water levels, 1350, 1450 and 1550 mm from the tank bottom

Examples of experimentally determined FFT spectra of transient time domain signals for the first set of fibre-based sensors (in fibre networks 1 to 4) on blade 1 and blade 5 are shown in Figure 8. A number of tests were conducted on the networks forming this set of fibre networks and these showed that the amplitudes of the individual FFT features depended on the location at which the blades were being excited. It was found that for this set of fibre networks, the optimum excitation location on the blades to capture the strong amplitudes and the natural frequencies in a single test lies somewhere between the centre line of the blade and trailing edge, close to the 0.9 radius position of the propeller. This was used in subsequent experiments.

A direct comparison was made of the results of the simulation and the experimental measurements, for each blade and for air and water, looking at the natural frequencies of vibration of the blade. This has resulted in a considerable volume of data, but here, for simplicity representative data are shown which illustrate the accuracy of the sensors used and thus the value of the approach.

Figure 9 shows a direct comparison of one of these representative sets of experimental and simulation results – this being obtained for blade 3 and acting as an illustration. The results show an excellent agreement for the first 12 natural frequencies, illustrating fully the capability of the specially designed optical FBG-based sensor network in capturing the vibration behaviour of a complex structure, such as a marine propeller. This has been done over a wide frequency range, at multiple positions, and both in air and water. This cannot be achieved with conventional sensors and under water.

Following the procedure explained in prior work from the authors [11], in order to investigate the mode orders, strain data captured from each sensor were plotted on an expanded area of the blade according to the sensor grid presented in Figure 3. Knowing the effective magnitude of strain and frequency at each location known, an interpolation of the strain data obtained from all the sensors at each natural frequency, has enabled the extensive 2D strain mode shapes shown (for blade

5) in Figure 10 to be created. The high number of sensors permitted using the optical approach has enabled this to be possible. Thus comparing the experimental and FE-based simulation results, it can be seen that excellent agreement between the two sets of data presented has been achieved. The optical FBG-based sensor network designed and used here has again showed itself to be the basis of a unique and reliable technique for the measurement of strains of full-sized marine propellers, both in water and in air.

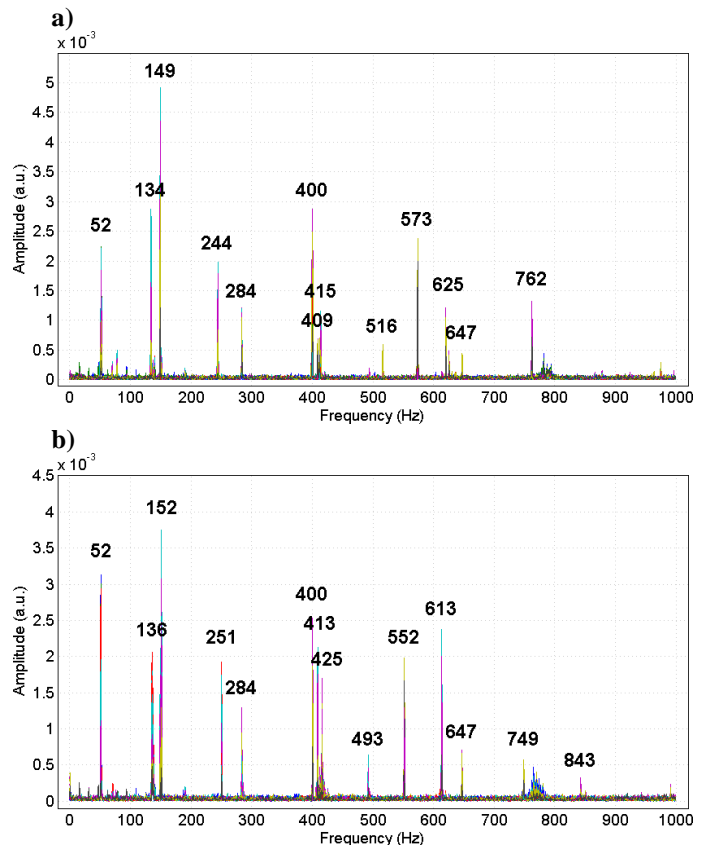


Fig. 8. FFT spectra calculated for captured signals from experimental tests in water on blade 1 (spectrum (a)) and blade 5 (spectrum (b)).

## V. CONCLUSION

A novel approach to the generation of accurate information for the analysis and thus better understanding of the displacement mode shapes of a full-sized actual marine propeller using a specially-designed optical fibre sensor network allowing monitoring in real-time of the associated Bragg wavelength shifts from arrays (networks) of FBG sensors has been reported. The results of simulation using finite element techniques with a theoretical model which was created using Abaqus FE software were verified through a comparison of the results obtained with those obtained through experimental measurements. The results were found to be in very good agreement, within experimental error. It was also confirmed that the location of the excitation on the blades, as expected, directly affected the amplitudes of the various frequencies that were detected in the experimental work.

The results of this work have shown the potential for the use of these advanced optically-based experimental techniques, coupled to advanced FE models to allow the most comprehensive investigation of actual multiple blade propellers of different types and sizes. This is the subject of on-going



research. However, clearly the outcome of this work has shown the value of innovative use of FBG-based sensor

networks for this purpose in different applications in marine technology.

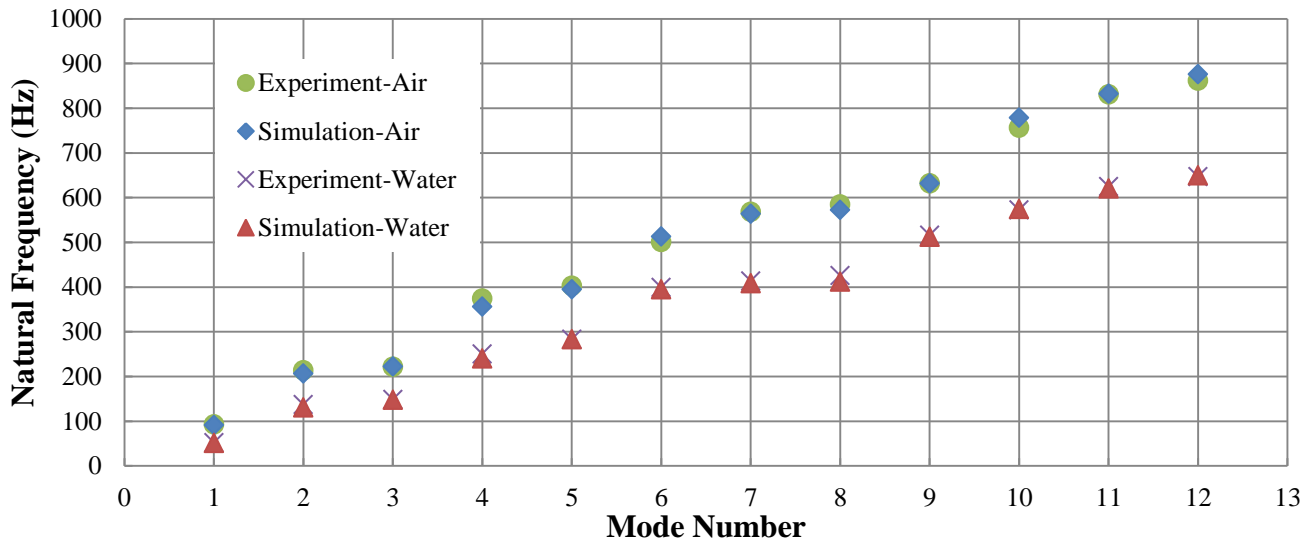


Fig. 9. Natural frequencies obtained from a series of tests, both experimental and simulation, both in air and in water, for blade 1.

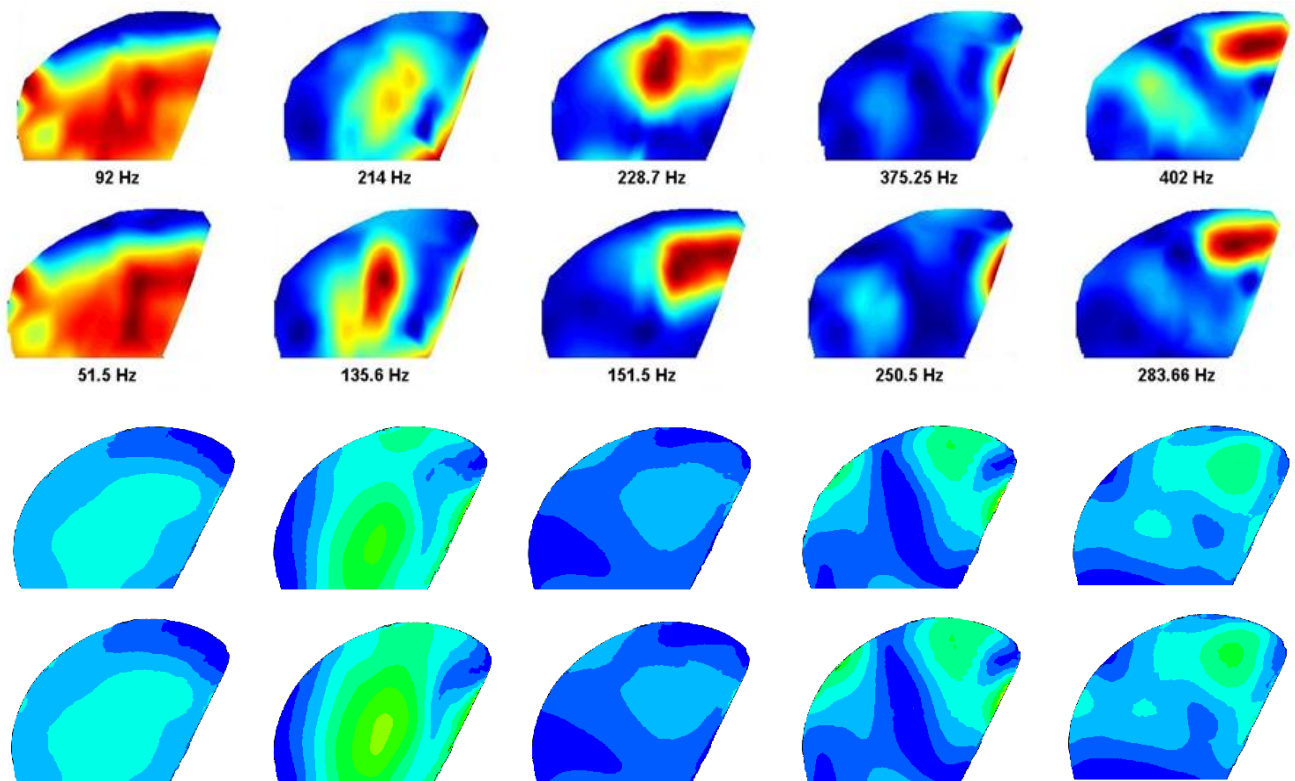


Fig. 10. First 5 natural frequencies strain mode shapes created from experimental data comparing to those obtained from FE analysis for blade 5. First row shows the strain mode shapes captured in air tests. Second row shows the results in water for the same blade. Third row shows the results of simulation in air and fourth row shows the calculated strain modes in water using Abaqus software for relatively similar natural frequencies.

#### ACKNOWLEDGMENTS

The support of the Royal Academy of Engineering and the George Daniels Educational Trust for K. T. V. Grattan is gratefully acknowledged.

#### REFERENCES

- [1] Conn, J.F.C. Marine propeller blade vibration. *Trans. IESS*, 1939.
- [2] P. Castellini and C. Santolini, Vibration measurements on blades of naval propeller rotating in water with tracking laser vibrometer, *Measurement*, 24, 43–54, 1998.
- [3] Carlton J. S., *Propeller blade vibration in Marine Propeller and Propulsion*, 3rd ed., Butterworth-Heinemann, Oxford, UK, 2012, ch. 21, pp. 421-429

- [4] Burrill, L. C., Underwater propeller vibration tests. *Trans. NECIES*, 65, 1949
- [5] Burrill, L. C., Marine propeller blade Vibrations: full scale tests. *Trans. NECIES*, 62, 1946
- [6] Hughes, W. L., Propeller blade vibrations. *Trans. NECIES*, 65, 1949
- [7] Lockwood Taylor, J., Propeller blade vibrations. *Trans. RINA*, 1945
- [8] Holden, K., Vibrations of marine propeller blades, *Norwegian Mar. Res.*, 3, 1974
- [9] K. O. Hill and G. Meltz, Fiber Bragg Grating Technology Fundamentals and Overview, *J. Lightwave Tech.* 15(8), pp. 1263-1276, 1997
- [10] O. C. Zienkiewicz, and R. E. Newton, "Coupled Vibrations of a Structure Submerged in a Compressible Fluid," *Symposium on Finite Element Techniques*, S 196 9, pp. 360-378.
- [11] S. Z. S. Javdani, M. Fabian, J. Carlton, T. Sun, K.T.V. Grattan, Fibre Bragg Grating-based system for measurement of vibrational characteristics of full-scale marine propeller blades, *J. International Shipbuilding Progress*, 2015, [to be published]

**Saeed Javdani** received his first M.S. degree from School of Engineering and Mathematical Sciences (SEMS), City University London, UK, in Maritime Operation and Management and his second M.S. degree in Maritime Transport and Economics from University of Antwerp, Belgium, in June and October 2011, respectively. He is currently pursuing his Ph.D. in mechanical engineering at SEMS, City University London, UK. His current research interests include vibration and transient signal analysis of marine structures using Fibre Bragg Grating (FBG) sensors.

**Matthias Fabian** Dr Matthias Fabian received a degree (Dipl.-Ing. (FH)) in Electronics from Hochschule Wismar, Germany, in 2006. He spent a semester at the Tokyo University of Science (TUS) in Tokyo, Japan, in 2005 gaining practical experience with microwave and optical devices. He was awarded his PhD in Fibre Optic Sensors from the University of Limerick, Ireland, in 2012. In 2010 he was awarded a short term visiting researcher grant from the Italian National Research Council for a stay at the National Institute of Optics in Naples, Italy, where he worked on fibre-loop cavity ringdown spectroscopy. He was a Systems Engineer intern at Intel Corporation for a year in 2011 writing software for wireless sensors connected to Android devices. He is currently a post-doctoral research fellow at City University London, UK, working on optical fibre sensors for a variety of applications in the civil engineering, marine and power electronics sector.

**John Carlton** Following training as a mechanical engineer and mathematician, Professor Carlton served in the Royal Naval Scientific Service undertaking research into underwater vehicle hydrodynamic design and propulsors. In 1975, he joined Lloyds Register, first in the Technical Investigation Department and after nine years transferred to the Advanced Engineering Department as its Deputy Head. He later moved to the newly formed Performance Technology Department where he initiated and led several research and development activities in the fields of ship hydrodynamics, diesel engine technology, machinery condition monitoring and control technology. In 1992 he returned to the Technical Investigation Department as the Senior Principal Surveyor and Head of Department in which capacity he served for 11 years and then, in 2003, Professor Carlton was invited to become the Global Head of Marine Technology for Lloyds Register.

After 35 years within Lloyds Register, Professor Carlton was then invited to become Professor of Marine Engineering at the City University London in which capacity he now serves and is responsible

for the postgraduate maritime studies. He is also closely involved with the newly formed International Institute for Cavitation Research at the University.

During his career he has presented and published around 120 technical papers and articles as well as having written a textbook entitled *Marine Propellers and Propulsion* which is now in its 3rd Edition. He is also a contributing author to the *Marine Engineering Reference Book*. Professor Carlton has been awarded the Denny Gold Medal of the Institute of Marine Engineering, Science and Technology twice and has also won the Stanley Gray Award for Marine Technology twice. Additionally, he is active in a number of research groups and has sat on several international and government committees. In 2006 he was awarded the honorary degree of Doctor of Science for his contribution to marine technology. Professor Carlton was the 109th President of the Institute of Marine Engineering, Science and Technology in 2011/12 and was elected a Fellow of the Royal Academy of Engineering in 2011.

**Tong Sun** Professor Tong Sun was awarded the degrees of Bachelor of Engineering, Master of Engineering and Doctor of Engineering from the Department of Precision Instrumentation of Harbin Institute of Technology, Harbin, China in 1990, 1993 and 1998 respectively. She was awarded the degree of Doctor of Philosophy at City University in applied physics in 1999 and was an Assistant Professor at Nanyang Technological University in Singapore from year 2000 to 2001 before she re-joined City University in 2001 as a Lecturer. Subsequently she was promoted to a Senior Lecturer in 2003, a Reader in 2006 and a Professor in 2008 at City University, London. Prof. Sun is currently the Director of Research Centre of Sensors and Instrumentation and is leading a research team focused on developing a range of optical fibre sensors for a variety of industrial applications, including structural condition monitoring, early fire detection, homeland security, process monitoring, food quality and environmental monitoring. She has been working closely with partners across disciplines from academia and industry, both in the UK and overseas. Prof. Sun is a member of the Institute of Physics and a Fellow of the Institution of Engineering and Technology and a Chartered Physicist and a Chartered Engineer in the United Kingdom. She has authored or co-authored some 230 scientific and technical papers.

**Kenneth T. V. Grattan** Professor Grattan graduated in Physics from Queens University Belfast with a BSc (First Class Honours) in 1974, followed by a PhD in Laser Physics in the use of laser-probe techniques for measurements on potential new dye laser systems. In 1978 he became a Research Fellow at the Imperial College of Science and Technology, to work on advanced photolytic drivers for novel laser systems. In 1983 he joined City University as a new blood Lecturer in Physics, being appointed Professor of Measurement and Instrumentation and Head of the Department of Electrical, Electronic and Information Engineering in 1991. His research interests have expanded to include the use of fibre optic and optical systems in the measurement of a range of physical and chemical parameters for industrial applications. He obtained a DSc from City University in 1992 for his work in sensor systems was President of the Institute of Measurement and Control during the year 2000. He was awarded the Callendar Medal and the Honeywell Prize of the Institute of Measurement and Control and was Dean of the School of Engineering & Mathematical Sciences and the School of Informatics at City University from 2008-12. He was appointed Dean of the City Graduate School in 2012. He was elected a Fellow of the Royal Academy of Engineering in 2008. He is the author of over seven hundred publications in major international journals and conferences and is the co-editor of a five volume topical series on Optical Fibre Sensor Technology.